IET Microwaves, Antennas & Propagation

Research Article

IET Journals
The Institution of Engineering and Technology

Reconfigurable resonant module for multi-band antenna design

ISSN 1751-8725
Received on 13th March 2015
Revised on 30th September 2015
Accepted on 5th October 2015
doi: 10.1049/iet-map.2015.0454
www.ietdl.org

Tsenchieh Chiu[1], Chichang Hung[1] ✉, Kaiming Hsu[2]

[1]*Department of Electrical Engineering, National Central University, Jhongli Dist., Taoyuan City 32001, Taiwan*
[2]*Department of Antenna, RF Business Unit, Walsin Technology Corp., No. 566-1, Gaoshih Rd., Yangmei Dist., Taoyuan City 32668, Taiwan*
✉ *E-mail: cchung1213@gmail.com*

Abstract: Novel resonant modules for constructing multi-band mobile antennas are proposed in this study. The basic configuration of the module, named as the prototype module, is designed based on a series LC resonant circuit. By adding a varactor to the module, it can be transformed into a reconfigurable module. By introducing an extra resonant mode with capacitive coupling to enhance the bandwidth, a wide-band module can be obtained. These modules have different frequency ranges, and can be combined into multi-band antennas for various applications. The proposed modules are demonstrated by constructing a 4G-LTE antenna. The reconfigurable module, which is of 20×20 mm^2, is designed to switch between LTE700 (698–787 MHz) and GSM850 (824–960 MHz) bands. The wide-band module, which is of 10×10 mm^2 and 49.3% bandwidth, is designed for GSM1800/GSM1900/UMTS/LTE2300/LTE2500 (1.71–2.59 GHz) applications. All designs have been realised and measured for validation. The proposed antenna modules, which are simple and convenient to use, can provide flexibility, especially in antenna deployment, in multi-band mobile antenna designs.

1 Introduction

Design of multi-frequency antenna for mobile communication applications has been attracting great interest. To accommodate many systems of different frequency into limited space, circuit components, including antennas, are often required to be multi-frequency and compact. There have been many multi-band antenna design schemes for mobile devices in the literatures. Among them, the intuitive method is to form the antenna by combining several resonators or resonant paths in the frequency bands of interest [1–4]. In [1], the antenna consists of multiple L- and U-shaped slots designed to resonate at the frequencies for WLAN/WiMAX applications. In [4], three slot monopoles are combined to form a multi-band antenna for WWAN applications. When using this design strategy, it is preferred that single resonator can cover as many frequency bands as possible, so the antenna volume can be compact without too many resonators.

To design, small resonators as the building blocks for multi-band antennas, in the circuit point of view, it is necessary to introduce sufficient inductance and capacitance in the compact structure, so it can resonate at the desired frequency. Zeroth-order resonant (ZOR) antenna design, based on the composite right/left-handed transmission line (CRLH-TL) [5–7], has been a rather systematic method for small antenna designs. The physical size and operational frequency of the ZOR antenna depend on the unit cell size and the transmission-line parameters including series inductance (L_R), series capacitance (C_L), shunt inductance (L_L) and shunt capacitance (C_R). In [8], a ZOR antenna is designed by using a short-ended CRLH-TL. With the short-circuited boundary condition, the antenna resonates at $\omega = 1/\sqrt{L_R C_L}$. In [9], the antenna is designed by using an open-ended CRLH-TL which resonates at $\omega = 1/\sqrt{L_L C_R}$. Like many small antennas, the ZOR antennas often suffer from narrow bandwidth. To enhance the antenna bandwidth, extra resonators have been added to the ZOR antenna to expand the bandwidth or create more frequency bands. In [10], a parasitic ring resonator is placed alongside the ZOR, and the bandwidth is enhanced from 240 to 840 MHz. In [11], the antenna comprises two resonators (a lower-band ZOR and a upper-band ZOR), so it can be used for GSM 850/1800/1900, WCDMA, and WiBro applications. Small antennas are inherently of narrow bandwidth. It is thus practical to combine multiple small resonators for wide-band [10] or multi-band [11, 12] antenna designs.

Reconfigurable technique [13–15] can also be applied to expand the frequency capability of the antenna. In multi-band systems, it is often that not all the frequency bands are in operation simultaneously. In the case, the reconfigurable antenna can be switched between different frequencies by using active components such as PIN diode and varactor. In [15], a dual-band reconfigurable antenna using two varactors is designed, and it can be switched among three GPS frequencies (1.227, 1.381 and 1.575 GHz). With the reconfigurable design, few antenna resonators are required. Nevertheless, it should be noted that the bias circuits for the active components should be carefully embedded in the antenna structure.

In this paper, convenient designs of resonant modules which can be used as building blocks to construct multi-band antennas are proposed. A prototype module is first introduced as the basic resonant unit. Unlike the ZOR designs in which the CRLH-TL is realised, the proposed module is designed by intuitively forming a simple series LC resonant circuit. The configuration of the prototype module can then be easily modified into two advanced modules for various applications: reconfigurable module and wide-band module. By replacing the edge-coupled capacitor with a varactor, the reconfigurable module can be obtained. The bias circuit for the varactor is embedded in the original structure, so the volume and radiation performance of the module is not significantly affected. To expand the bandwidth of the prototype module, an extra resonant mode is introduced by placing a coupling patch under the module, and the wide-band module is thus obtained.

In Section 2, the design of the prototype module will be explained and experimentally validated. In Section 3, how to modify the prototype module into the reconfigurable module and wide-band module will be explained. Both modules will be combined into a multi-band antenna for 4G-LTE applications. The reconfigurable module will be designed to switch between LTE700 and GSM850 bands, while the wide-band module will be designed to operate in

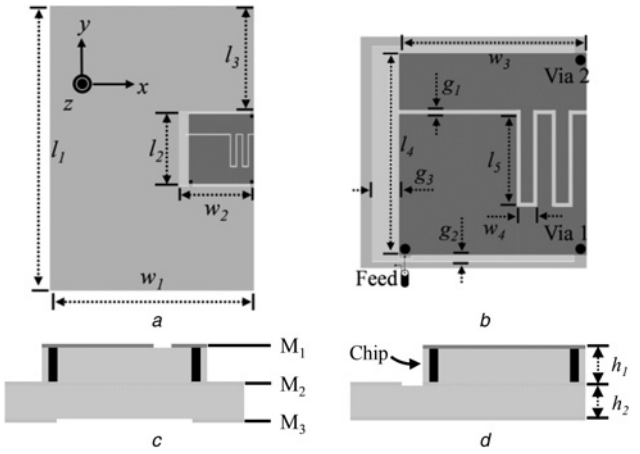

Fig. 1 *Configuration of the prototype module*

a Module is deployed along the edge of PCB
b Top view of the module
c Side view by looking into the $-\hat{x}$ direction. M_1, M_2 and M_3 denote the three metallic layers
d Side view by looking into the $\hat{y}$ direction. Both dielectric thicknesses, h_1 and h_2, are 0.8 mm

Table 1 Dimensions (mm) of the prototype module in Fig. 1

l_1	l_2	l_3	l_4	l_5	w_1	w_2
160	15	73	14	6.6	80	15
w_3	w_4	g_1	g_2	g_3	h_1	h_2
12.6	1.5	0.4	0.5	2	0.8	0.8

GSM1800/GSM1900/UMTS/LTE2300/LTE2500 bands. Both reconfigurable and wide-band modules will be realised and measured for validation. The conclusions will be given in Section 4.

2 Design of prototype module

In this section, the design of the prototype antenna module is described. The prototype module will be modified into reconfigurable module and wide-band module in the following section. These modules are designed and fabricated on the FR4 printed circuit board (PCB) with dielectric constant of 4.4 and loss tangent of 0.0125. The module is deployed along the edge of PCB, as shown in Fig. 1*a*. There are three metal layers in the PCB, as shown in Figs. 1*c* and *d*. The antenna is design in the top two layers, M_1 and M_2. It can also be considered that an antenna chip is attached on the ground plane (M_3). The antenna is fed by a 50 Ω coaxial cable. The full-wave and circuit simulations in the design are carried out by using high frequency structure simulator (HFSS) [16] and advanced design system (ADS) [17], respectively.

Fig. 1*b* shows the proposed configuration of the prototype module. The motivation of the design is to intuitively construct the module like a simple series LC circuit. The capacitance is provided by the interdigital-coupled capacitor [18] in the middle of the module. The value of capacitance can be adjusted by changing the gap distance, finger length and the number of fingers of the capacitor. The inductance is mainly provided by the edges (l_4 and w_3) and the grounding via (Via 2). An example of module at 850 MHz is designed, and the dimensions are given in Table 1. Fig. 2*a* shows the simulated current distribution over the module at 850 MHz. It can be seen that the currents distribute mainly around the capacitor and along the l_4 and w_3 edges and Via 2. The current is also found around Via 1. The role of Via 1 is to provide a tuning mechanism for impedance matching, and ground the module in static state which is essential to the later reconfigurable design. With the

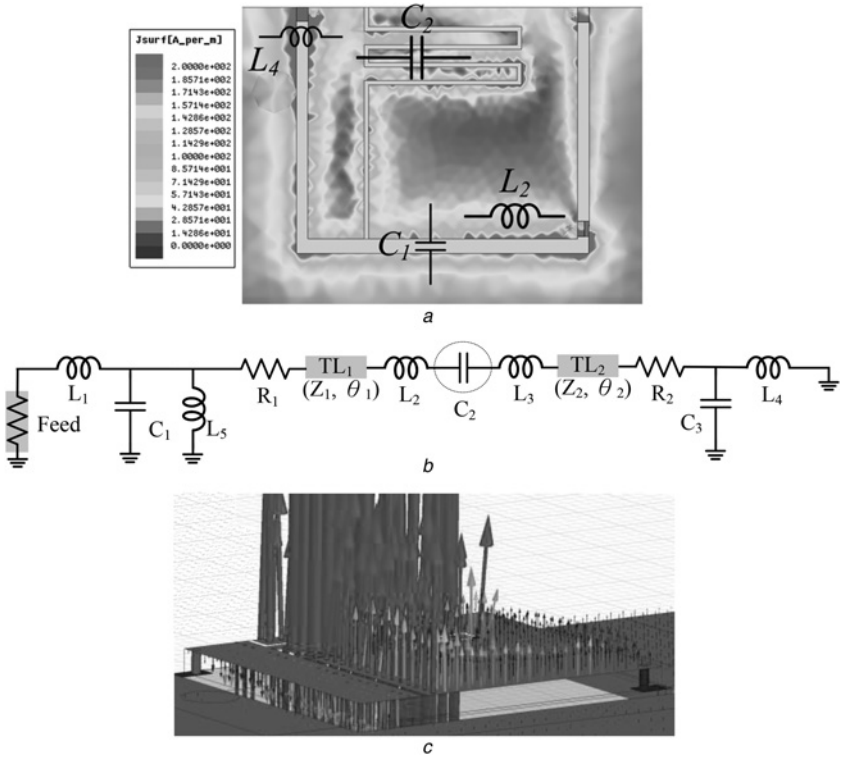

Fig. 2 *Equivalent circuit and HFSS simulation results for the prototype module in Fig. 1b*

a Simulated current distribution
b Equivalent circuit
c Simulated electric field distribution

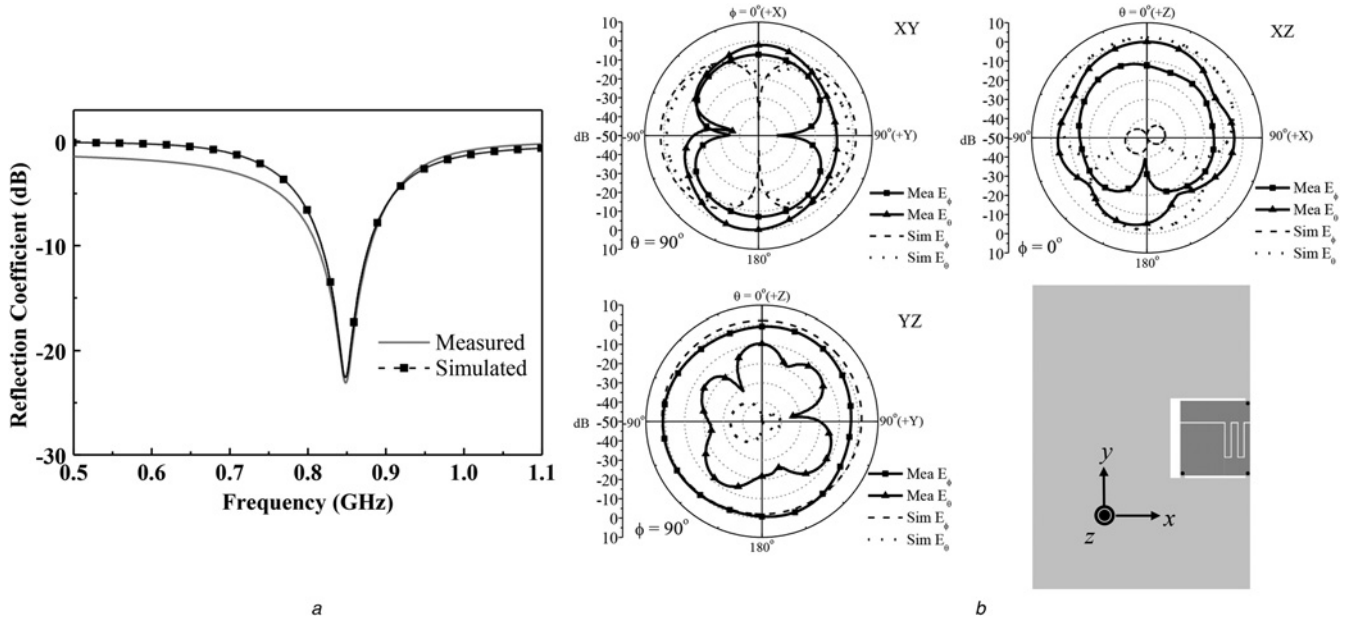

Fig. 3 *Simulated and measured results for the module in Fig. 1b at 850 MHz*

a Simulated and measured reflection coefficients
b Simulated and measured radiation patterns

current distribution in Fig. 2*a*, the detailed equivalent circuit of the module is developed in Fig. 2*b*. In the circuit, C_2 represents the interdigital capacitor in the middle, while other components account for the effects of the edges (C_1, C_3, L_1, L_2, L_3 and L_4), Vias (L_1, L_4 and L_5) and radiation (R_1 and R_2). Though the proposed design looks like a short-ended ZOR antenna, there are some differences need to be noted. While the resonance frequency of the short-ended ZOR is determined by L_R and C_L, it is found that the variation of almost all components of the circuit in Fig. 2*b* are related to the resonant frequency. Fig. 2*c* shows the electric field distribution over the module. It is found that the magnitude of the field is highly non-uniform and there is phase difference across the inter-digital capacitor, which is not ZOR characteristic.

The design in Fig. 1*b* is realised and measured for validation. Fig. 3 shows the simulation and measured reflection coefficients and patterns for the prototype module at 850 MHz. The measurements of reflection coefficients are conducted by using a vector network analyser E8362B [19], and the patterns are measured in an anechoic chamber. The measurement shows that the prototype module is able to resonate at 850 MHz with 15.4% bandwidth (defined with −6 dB reflection coefficient), 84% in efficiency, 1.44 dBi in peak gain and an area of 15×15 mm^2 ($0.042 \times 0.042\ \lambda_0^2$). Therefore, the design is a capable radiator.

Fig. 4*a* shows the circuit simulation for the antenna in Fig. 1 with various values of C_2. As expected, the centre frequency is decreased as C_2 is increased. Meanwhile, the bandwidth (based on the reflection coefficient of −6 dB) is decreased from 14.2 to 9.4%. The size of the ground plane can also affect the performance of the antenna. Fig. 4*b* shows the full-wave simulation for the

Table 2 Dimensions (mm) of the reconfigurable module in Fig. 6

g_4	g_5	l_6	l_7	l_8	l_9	l_{10}	l_{11}
0.9	2	20	11	18	1.5	2	5.4
w_5	w_6	w_7	w_8	w_9	w_{10}	w_{11}	w_{12}
75	42	20	10	19	3.1	2	1.6

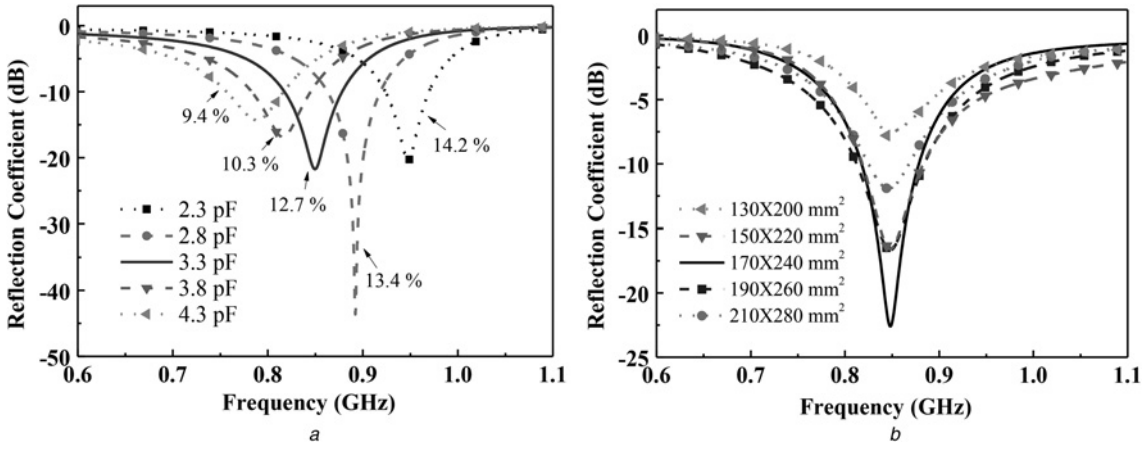

Fig. 4 *Simulated results for the effect of the capacitance (C_2) and the PCB size in Fig. 1b*

a Simulated effect of the capacitance (C_2) on the bandwidth for the module in Fig. 1*b*. C_2 is varied and the other parameters are listed in Table 2
b Simulated effect of the PCB size on the module in Fig. 1*b*. In the simulation, the values of w_1 and l_1 are varied

antenna in Fig. 1 with various areas of the ground plane. It is found that changing the ground plane area mainly affects the impedance matching, while the centre frequency is hardly shifted. In addition, it is found that, as the ground plane area is decreased, the bandwidth of the antenna is also decreased. Both simulations in Fig. 4 indicate that insufficient bandwidth would be of concern if an antenna of low frequency is designed on a small ground plane.

3 Reconfigurable module and wide-band module for multi-band applications

In this section, the prototype module will be modified into two modules, reconfigurable module and wide-band module. Both modules are combined to form a multi-band 4G-LTE antenna. The spectrum of the antenna is divided into the lower-band including LTE700 (698–787 MHz, 12%) and GSM850 (824–960 MHz, 15.2%), and the upper band covering all GSM1800/GSM1900/UMTS/LTE2300/LTE2500 (1.71–2.59 GHz, 45.6%). The reconfigurable module is designed to switch between LTE700 and GSM850, while the wide-band module is designed for the upper-band operation. As shown in Fig. 5*a*, both modules are deployed along the narrow edge of the PCB. These modules can be combined together by using a miniature diplexer, Mini-Circuit LDP-1050-252+ [20], which is of $3.2 \times 1.6 \times 0.8$ mm^3. The positions of both modules should be carefully chosen to avoid undesired mutual coupling.

3.1 Reconfigurable design

When designing miniature 4G-LTE antennas, the difficulty often lies in determining the resonant structures for LTE700 and GSM850 bands due to the low centre frequencies and required fractional bandwidths. Since both bands are close to each other in frequency spectrum and the required bandwidths are similar, the reconfigurable design is a good choice, in which both bands can use the same antenna structure. The configuration shown in Fig. 1*b* can be easily adapted to become a reconfigurable one by placing a varactor across the middle slot. Fig. 6 shows the proposed configuration of the reconfigurable module for LTE700/GSM850. The module is deployed on the upper edge of the PCB, along with the wide-band module which will be explained later. To obtain sufficient bandwidth for LTE700 and GSM850, an area of 20×20 mm^2 (0.056×0.056 λ_0^2 at 850 MHz) is chosen, so larger capacitance of varactor, which could result in the bandwidth reduction, will not be required.

The varactor (C_V in Fig. 6*a*) requires the bias voltage to operate. However, the prototype structure in Fig. 1*b* is of equal potential in steady state, since the whole structure is connected to the ground plane through Vias 1 and 2. To create static potential difference over the antenna structure in steady state, a capacitor, C_{dc}, shown in Figs. 6*a* and *b*, is used as a DC block. The value of C_{dc} (20 pF) is large, so it is able to block the direct current while the RF signal of interest is hardly affected. The point P in Fig. 6*b* is connected to a 1 K Ω resistor (R) as shown in Fig. 6*c*. The bias voltage is applied at V_{bias} as shown in Fig. 6*a*. The open voltage at point P is the same as V_{bias}. The resistor serves as an RF choke to prevent RF currents from flowing through the DC path, so the bias voltage variation caused by interference can be lessened. The bias circuit for the varactor is embedded in the antenna structure, and it does not require extra space for antenna design. Through numerical simulation, it has been checked that the presence of the bias circuit hardly affects the RF performance of the antenna.

The centre frequency of the module can be adjusted by tuning the voltage difference across the varactor. Fig. 7 shows the measured capacitance versus applied voltage for the varactor MA46H120 [21] used in the design. By changing the bias voltage according to Cases #1 and #2 in Table 3, the module can be switched between LTE700 and GSM850 bands, respectively. As shown in Fig. 7, the varactor in both cases is not operated in the saturation state (in which the bias voltage is larger than about 5 V), so it provides sufficient sensitivity of capacitance to the variation of the bias

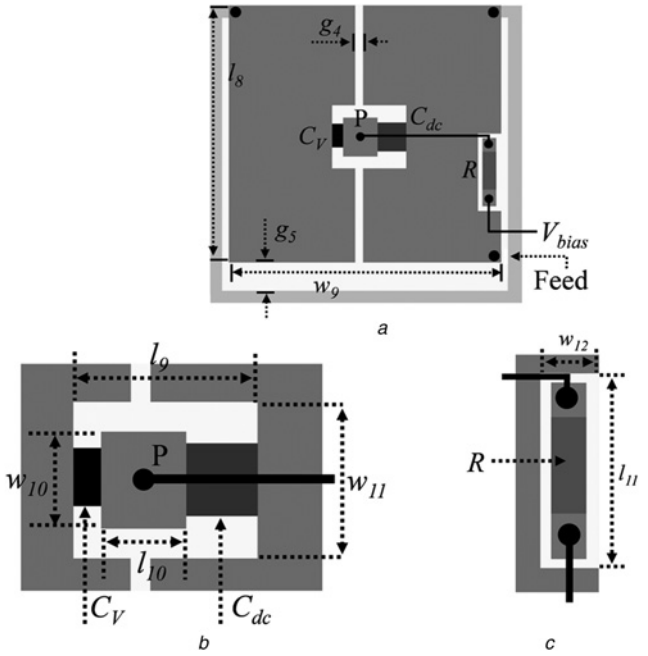

Fig. 6 *Reconfigurable module for LTE700/GSM850*

a Module configuration and parameters are listed in Table 2
b Deployment of the varactor and the DC block (C_{dc}). Both are in dark colour
c RF choke (R) in dark colour and the feed of the bias voltage (V_{bias})

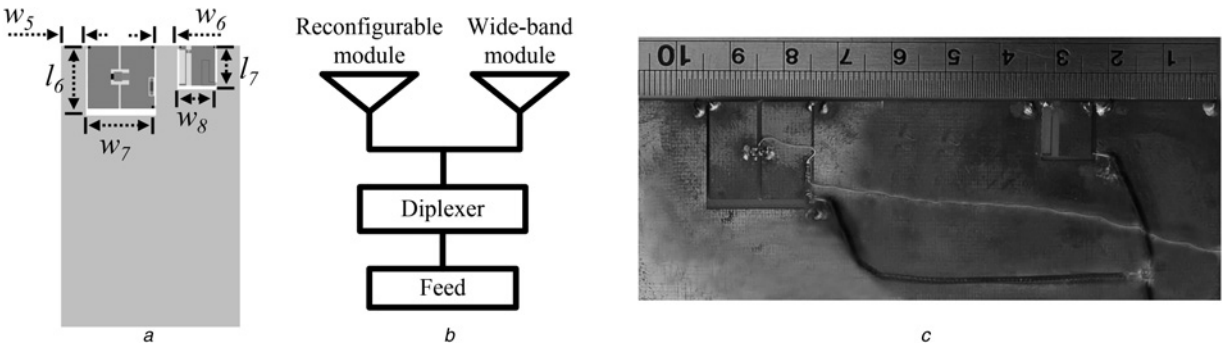

Fig. 5 *Module deployment and photography for the 4G-LTE antenna*

a Reconfigurable module in the left and wide-band module in the right. w_5 and w_6 denote the spacings
b Both modules can be combined by a miniature LTCC diplexer
c Photography of the fabricated 4G-LTE antenna

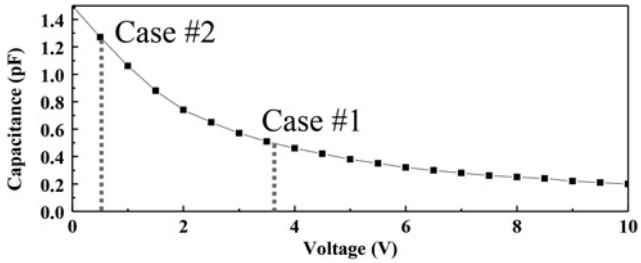

Fig. 7 *Measured capacitance versus applied voltage for the varactor MA46H120 [21]*

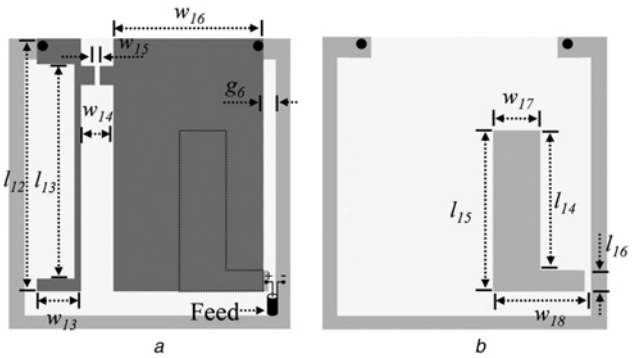

Fig. 10 *Configuration of the wide-band module*

a Top view
b View of the M_2 layer
Dimensions are given in Table 4

voltage (V_{bias}). The simulated and measured reflection coefficients for both Cases #1 and #2 are shown in Fig. 8*a*, in which the measured bandwidths are 668–816 MHz (20.3%) for LTE700 and 811–983 MHz (19%) GSM850. The simulation and measurement of antenna efficiency, peak gains and antenna patterns are also conducted and shown in Fig. 8*b* and Fig. 9, respectively. It is found that the measured antenna efficiency is larger than 80% in

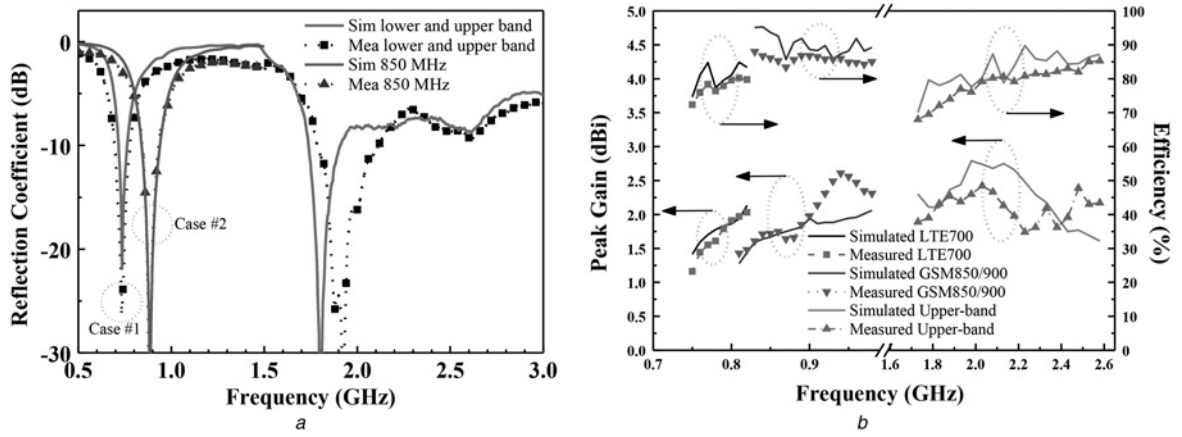

Fig. 8 *Simulated and measured results for the antenna in Fig. 5*

a Reflection coefficient. Bias voltages and capacitance for Cases #1 and #2 are given in Table 3
b Peak gain and efficiency

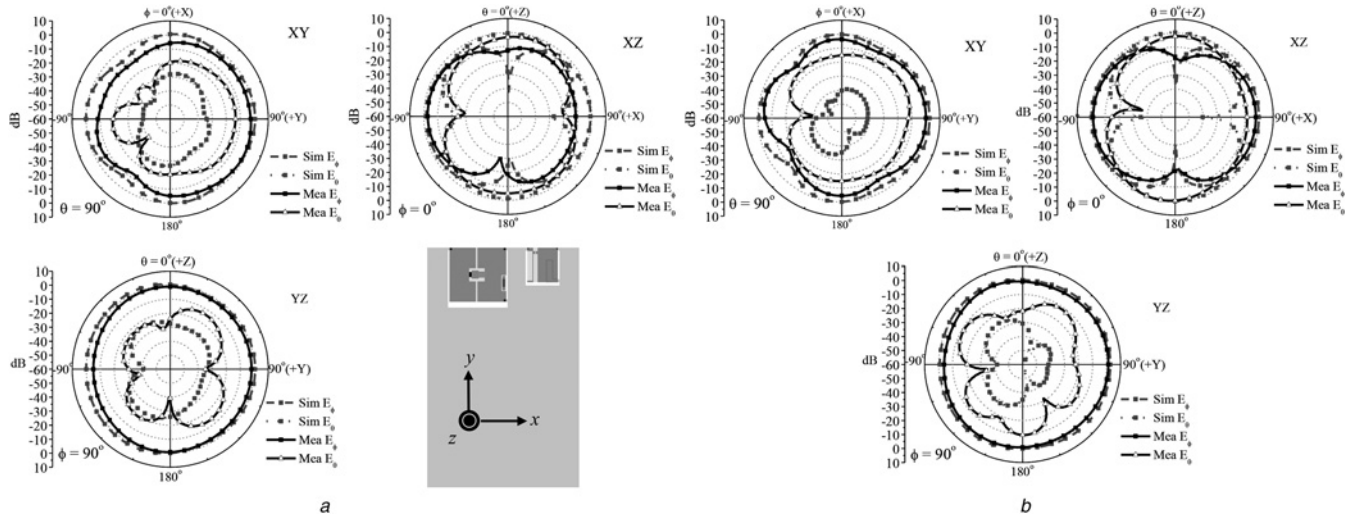

Fig. 9 *Simulated and measured antenna patterns for the reconfigurable module in Fig. 6*

a 734 MHz
b 884 MHz

Table 3 Values of bias voltage and varactor

	Case #1	Case #2
C_V, pF	0.92	0.42
V_{bias}, V	0.52	3.62

Table 4 Dimensions (mm) of the wide-band module in Fig. 10

g_6	l_{12}	l_{13}	l_{14}	l_{15}	l_{16}
0.5	10	8.5	5.7	6.5	0.8
w_{13}	w_{14}	w_{15}	w_{16}	w_{17}	w_{18}
1.75	1.3	0.2	5.95	1.9	3.3

LTE700 band and 85% in GSM850 band. Even with the additional insertion loss of the diplexer, the antenna possesses sufficient gain. Also the patterns indicate that there is no blind angle in radiation.

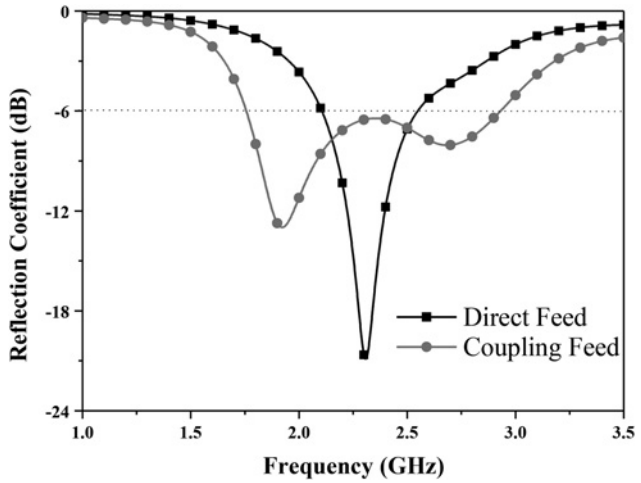

Fig. 11 *Simulated reflection coefficients for the modules with direct feed and capacitive-coupling feed*

3.2 Wide-band design

In the prototype and reconfigurable designs, the bandwidths are only about 20%, which is not sufficient to cover the upper band (1.71–2.59 GHz and 45.6%). Therefore, a bandwidth-enhanced module will be proposed. Generally, the bandwidth enhancement can be achieved by introducing an extra mode into original module. In the proposed design, it is done by using the capacitive coupling at the input terminal to introduce another resonance into the prototype module. Fig. 10 shows the configuration of the 10×10 mm^2 (0.073×0.073 λ_0^2 at 2.2 GHz) wide-band module. Basically, the configuration in Fig. 10*a* is similar to that the prototype module in Fig. 1*b*, except that a folded edge (at l_{12}) is used to increase the inductance and make the module resonate in the upper band. As shown in Fig. 10*b*, the input signal is first applied across the slot between the ground plane and L-shape patch, and then coupled to the antenna through the capacitor formed by the antenna and patch. The effect of the coupling patch can be observed in the simulation is shown in Fig. 11. When the signal is directly connected to the antenna without the patch, as is done in the prototype module, there is only one resonance at 2.3 GHz with 20.2% bandwidth. With the coupling patch, there are two resonant modes at 1.93 and 2.72 GHz. The combined bandwidth of both modes is about 49.3%, which is sufficient for the applications of interest. The wide-band module is deployed along with the reconfigurable modules, as shown in Fig. 5*a*. The distance between both modules has been carefully chosen, so the mutual-coupling effect is insignificant. The simulated and measured reflection coefficients of the wide-band module are shown in the right side of Fig. 8*a*. Due to the manufacturing deviation in circuit realisation, the pole at 1.8 GHz in simulation is shifted to 1.88 GHz in measurement. Nevertheless, the measured bandwidth is wide enough for the applications of interest. The simulation and measurement of antenna peak gains, efficiency and patterns are shown in Fig. 8*b* and Fig. 12, respectively. It is found that the measured antenna efficiency is larger than 70% in the upper band.

As mentioned previously and seen in many literatures, many multi-band antenna designs have been basically the combinations of multiple resonators. Similarly, the reconfigurable and wide-band modules are combined into a single multi-band antenna via a miniature diplexer. Fig. 13*a* demonstrates combinations of three different deployments. Fig. 13*b* shows that these different deployments possess similar performance of reflection coefficient. The total volume of the proposed 4G-LTE antenna is about 405

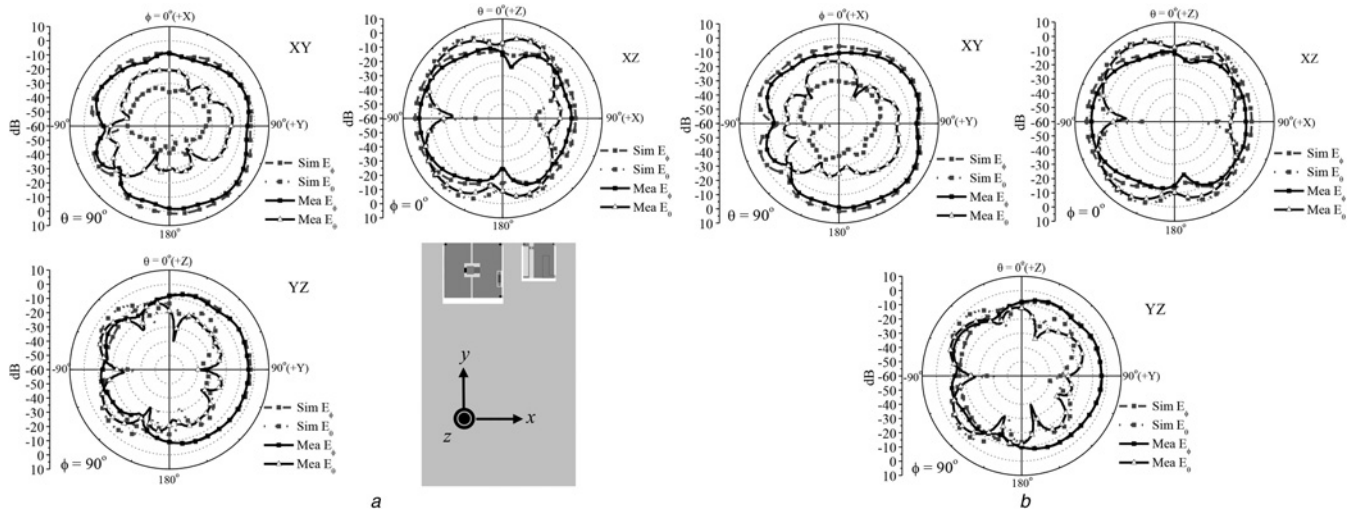

Fig. 12 *Simulated and measured antenna patterns for the wide-band module in Fig. 10*

a 1.89 GHz
b 2.36 GHz

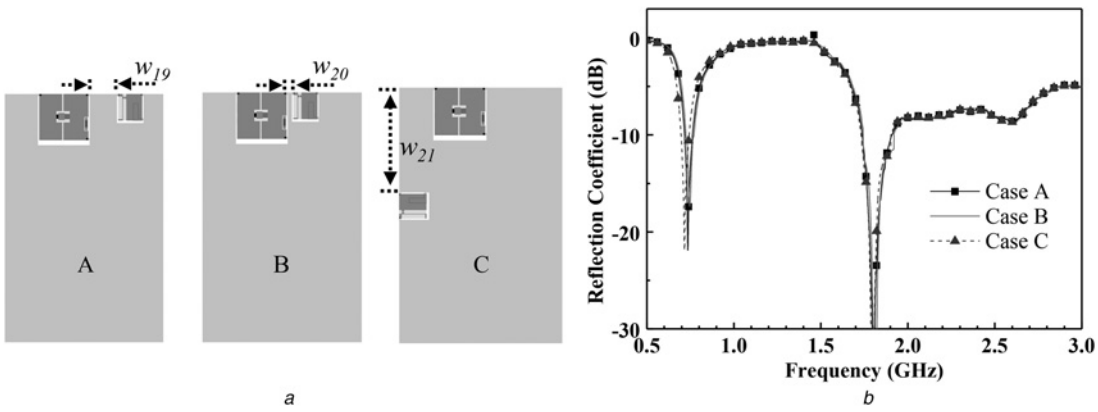

Fig. 13 *Comparison of the antenna response with different module deployments*

a Three cases of deployment w_{19}, w_{20} and w_{21} are 42, 10 and 120 mm, respectively
b Simulated reflection coefficient

mm^3. Considering the comparison provided by Wong and Liao [22] in which the volume of the various 4G-LTE antennas ranges from 280 to 1200 mm^3, it is found the size of the proposed design is reasonable, yet provided great flexibility in antenna deployment.

4 Conclusion

Novel resonant modules for constructing multi-band mobile antennas have been proposed in this paper. The basic configuration of the module, named as the prototype module, is designed based on a series LC resonant circuit. The design consideration and analysis have been described, including structure explanation, simulations of current distribution and antenna parameters, and measurements. By adding a varactor to the module, it is transformed into a reconfigurable module. By introducing an extra resonant mode with capacitive coupling to enhance the bandwidth, a wide-band module is obtained. A multi-band antenna can be constructed by combining these modules. In this paper, a 4G-LTE antenna is designed for demonstration. The reconfigurable module, which is of 20×20 mm^2, is designed to switch between LTE700 (698–787 MHz) and GSM850 (824–960 MHz) bands. The wide-band module, which is of 10×10 mm^2 and 49.3% bandwidth, is designed for GSM1800/GSM1900/UMTS/LTE2300/LTE2500 (1.71–2.59 GHz) applications. All designs have been realised and measured for validation. The total volume of the proposed 4G-LTE antenna is about 405 mm^3, which is reasonable considering the volume of the various 4G-LTE antennas ranges from 280 to 1200 mm^3 [22]. The proposed antenna modules, which are simple and convenient to use, can provide flexibility, especially in antenna deployment, in multi-band mobile antenna designs [23–25].

5 Acknowledgments

This work was supported by the Ministry of Science and Technology R.O.C., under Grant NSC 101-2221-E-008-084.

6 References

1 Moosazadeh, M., Kharkovsky, S.: 'Compact and small planar monopole antenna with symmetrical L- and U-shaped slots for WLAN/WiMAX applications', *IEEE Antennas Wirel. Propag. Lett.*, 2014, **13**, pp. 388–391
2 Cao, Y.F., Cheung, S.W., Yuk, T.I.: 'A multiband slot antenna for GPS/WiMAX/WLAN systems', *IEEE Trans. Antennas Propag.*, 2015, **63**, (3), pp. 952–958
3 Liu, H.J., Li, R.L., Pan, Y., *et al.*: 'A multi-broadband planar antenna for GSM/UMTS/LTE and WLAN/WiMAX handsets', *IEEE Trans. Antennas Propag.*, 2014, **62**, (5), pp. 2856–2860
4 Wong, K.L., Lee, L.C.: 'Multiband printed monopole slot antenna for WWAN operation in the laptop computer', *IEEE Trans. Antennas Propag.*, 2009, **57**, (2), pp. 324–330
5 Lai, A., Caloz, C., Itoh, T.: 'Composite right/left-handed transmission line metamaterials', *IEEE Microw. Mag.*, 2004, **5**, (3), pp. 34–50
6 Lee, C.J., Leong, K.M.K.H., Itoh, T.: 'Composite right/left-handed transmission line based compact resonant antennas for RF module integration', *IEEE Trans. Antennas Propag.*, 2006, **54**, (8), pp. 2283–2291
7 Ueda, T., Michishita, N., Akiyama, M., *et al.*: 'Dielectric-resonator-based composite right/left-handed transmission lines and their application to leaky wave antenna', *IEEE Trans. Microw. Theory Tech.*, 2008, **56**, (10), pp. 2259–2269
8 Chi, P.L., Shih, Y.S.: 'Compact and bandwidth-enhanced zeroth-order resonant antenna', *IEEE Antennas Wirel. Propag. Lett.*, 2015, **14**, pp. 285–288
9 Ko, S.T., Lee, J.H.: 'Hybrid zeroth-order resonance patch antenna with broad E-plane beamwidth', *IEEE Trans. Antennas Propag.*, 2013, **61**, (1), pp. 19–25
10 Wang, G., Feng, Q.: 'A novel coplanar waveguide feed zeroth-order resonant antenna with resonant ring', *IEEE Antennas Wirel. Propag. Lett.*, 2014, **13**, pp. 774–777
11 Ji, J.K., Kim, G.H., Seong, W.M.: 'A compact multiband antenna based on DNG ZOR for wireless mobile system', *IEEE Antennas Wirel. Propag. Lett.*, 2009, **8**, pp. 920–923
12 Li, L., Jia, Z., Huo, F., *et al.*: 'A novel compact multiband antenna employing dual-band CRLH-TL for smart mobile phone application', *IEEE Antennas Wirel. Propag. Lett.*, 2013, **12**, pp. 1688–1691
13 Khidre, A., Yang, F., Elsherbeni, Z.: 'A patch antenna with a varactor-loaded slot for reconfigurable dual-band operation', *IEEE Trans. Antennas Propag.*, 2015, **63**, (2), pp. 755–760
14 Tariq, A., Ghafouri-Shiraz, H.: 'Frequency-reconfigurable monopole antennas', *IEEE Trans. Antennas Propag.*, 2012, **60**, (1), pp. 44–50
15 Hung, C., Chiu, T.: 'Dual-band reconfigurable antenna design using slot-line with branch edge', *IEEE Trans. Antennas Propag.*, 2015, **63**, (2), pp. 508–516
16 High frequency structure simulator (HFSS), version, 13, ANSYS Inc.
17 Advanced design system (ADS), version, 2009, Agilent Technologies
18 'Over view on interdigital capacitor design', http://www.cp.literature.agilent.com/litweb/pdf/5989-8912EN.pdf, accessed 18 June 2015
19 'Agilent network analyzer PNA E8362B', http://www.literature.cdn.keysight.com/litweb/pdf/5988-7988EN.pdf?id=1000084422:epsg:dow, accessed 9 March 2015
20 'Mini-Circuits', http://www.minicircuits.com/pdfs/LDP-1050-252+.pdf, accessed 15 January 2015
21 'M/A-COM Technology Solutions Inc.', http://www.macomtech.com/datasheets/MA46H120.pdf, accessed 20 April 2014
22 Wong, K.L., Liao, Z.G.: 'Passive reconfigurable triple wideband antenna for LTE tablet computer', *IEEE Trans. Antennas Propag.*, 2015, **63**, (3), pp. 901–908
23 Lu, J.H., Wang, Y.S.: 'Planar small-size eight-band LTE/WWAN monopole antenna for tablet computers', *IEEE Trans. Antennas Propag.*, 2014, **62**, (8), pp. 4372–4377
24 Wong, K.L., Chen, M.T.: 'Small-size LTE/WWAN printed loop antenna with an inductively coupled branch strip for bandwidth enhancement in the tablet computer', *IEEE Trans. Antennas Propag.*, 2013, **61**, (12), pp. 6144–6151
25 Sung, Y.: 'Simple inverted-F antenna based on independent control of resonant frequency for LTE/wireless wide area network applications', *IET Microw. Antennas Propag.*, 2015, **9**, (6), pp. 553–560